

CO-SEISMIC LANDSLIDE BASED VALIDATION OF SUSCEPTIBILITY MAPPING AFTER KAHRAMANMARAS EARTHQUAKES (FEB 6, 2023) IN AMANOS MOUNTAINS

G. Karakas^{1,2}, E.O. Unal¹, N. Tunar Ozcan³, S. Cetinkaya¹, R. Can¹, C. Gokceoglu³, S. Kocaman^{2,*}

¹ Hacettepe University, Graduate School of Science and Engineering, Ankara, Türkiye – gizem.karakas@hacettepe.edu.tr, erdincunal@hacettepe.edu.tr, sinemcetinkaya@hacettepe.edu.tr, recepcan@hacettepe.edu.tr

² Dept. of Geomatics Engineering, Hacettepe University, 06800 Beytepe Ankara, Türkiye - sultankocaman@hacettepe.edu.tr

³ Dept. of Geological Engineering, Hacettepe University, 06800 Beytepe Ankara, Türkiye - ntunar@hacettepe.edu.tr, cgokce@hacettepe.edu.tr

KEY WORDS: Landslide Susceptibility Mapping, Random Forest, Aerial Photogrammetry, Validation, Kahramanmaras Earthquakes (6 Feb 2023)

ABSTRACT:

The quality of landslide susceptibility maps is often assessed using a part of learning data that represents geographical and land use characteristics over a quasi-fixed time. However, when validated with multi-temporal landslide inventories, more realistic insights on the susceptibility maps can be obtained. In addition, extreme events may trigger landslides in regions which are not considered as landslide-prone. The February 6, 2023, Kahramanmaras Earthquakes (Mw 7.7 and Mw 7.6), also known as the disaster of the century, triggered numerous landslides. Amanos Mountains located in southern Türkiye were also within the earthquake-affected area and had a very small amount of inventory recorded in official databases. The aim of this study was to evaluate the performance of the random forest method for producing landslide susceptibility maps. The official inventory of General Directorate of Mineral Research and Exploration (MTA) was used for map production. The resulting susceptibility map was assessed using the co-seismic landslide inventory produced in the study. The model's performance evaluated using a part of the learning data yielded high accuracy expressed with area under receiver operating characteristics curve (AUC), precision, and recall values and F1 score using (AUC = 97%, recall = 97%, precision = 96%, F1 = 98%). However, multi-temporal evaluation with co-seismic landslides showed that 80% of the landslide pixels with moderate, high, and very high susceptibility levels could be predicted with the model. The results suggest that special attention should be given to features underrepresented in the inventory, such as low altitudes and types of lithology.

1. INTRODUCTION

Landslides have devastating effects on settlements, infrastructure, and other natural and economic resources. Identification of landslides requires a high level of expertise in geology and topography. High-quality geospatial datasets enable the use of data-driven machine learning (ML) methods for landslide hazard assessments and reduce the limitations derived from field inaccessibility. As a first step in landslide disaster management, the question of “where” should be answered. Landslide susceptibility mapping aims to answer this question. Although novel ML methods and freely available geodata provide new opportunities in precision and computation cost, the main challenges remain in the availability of accurate inventories to be used as learning data and reliable quality assessment and validation approaches.

In recent decades, natural hazards, including earthquakes, landslides, and avalanches, have exhibited a significant influence on the lives of people all over the globe. Landslides can be triggered by other natural hazards, including earthquakes (Karakas et al., 2021; Shao and Xu, 2022) and heavy rainfalls (Kocaman et al., 2020), or anthropogenic activities (Sevgen et al., 2019; Yanar et al., 2020). An earthquake can trigger landslides in areas with unstable slopes or hills. The shaking from an earthquake can destabilize the soil or rock on a slope, causing it to fail and slide downhill. The likelihood of a

landslide occurring during an earthquake depends on several factors, such as the slope gradient, the type and properties of the soil or rock, the water content of the soil, and the magnitude and duration of the earthquake. Slopes with steeper gradients are usually more susceptible to sliding during an earthquake, as are those with weaker or less cohesive soil or rock types.

Several types of earthquake-induced landslides can be listed, such as circular or translational failures, rock falls, rock avalanches, debris flows, mudflows, sackung, etc. Besides the damages caused by the earthquake event, landslides can lead to significant damage to infrastructure and property, as well as pose a serious threat to human life. The Kahramanmaras earthquakes (Mw 7.7 and Mw 7.6) occurred on 6 February 2023 triggered numerous landslides of those types. A selection of the co-seismic landslides triggered by this event can be seen in Figure 1. Almost 3000 co-seismic landslides were identified by several research groups, including ours. However, a great majority of them was not included in the official databases of General Directorate of Mineral Research and Exploration (MTA).

Production of accurate and up-to-date susceptibility maps with data-driven ML methods requires high-quality inventories. However, the inventories may be incomplete for several reasons. The requirements of a high level of expertise and site inaccessibility are among the two main ones. Karakas et al.

(2021) compiled an inventory of landslides triggered after the Elazig earthquake (the January 24, 2020, Mw 6.8). A total of 328 landslides were identified from the 3D models and high resolution orthophotos. A volumetric change detection was also carried out using aerial photogrammetric datasets in the same study, which revealed the importance and usability of pre- and post-event data for an in-depth analysis of the landslide characteristics (even very small ones).

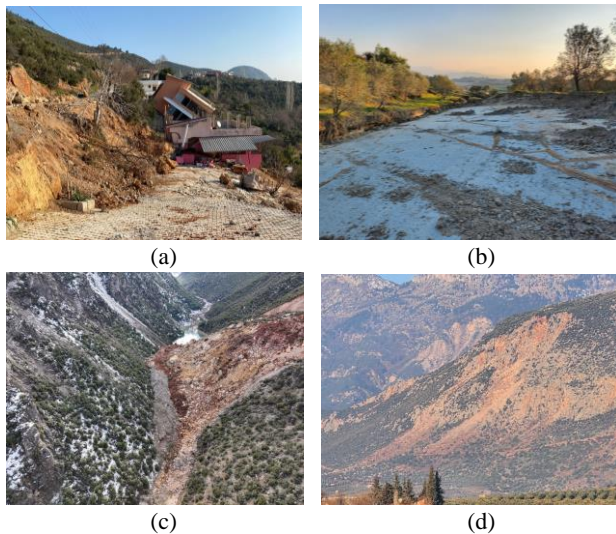


Figure 1. Examples to co-seismic landslides in the study area; (a) rock mass failure, (b) planar failure developed in gentle slope topography, and (c) and (d) circular failure.

The landslide susceptibility assessment methods are diverse. Shao and Xu (2022) provided a comprehensive review of the current state-of-the-art in landslide susceptibility assessment for earthquake-induced landslides and highlighted the need for continued research and development in this area. This review also discussed the challenges and limitations of landslide susceptibility assessment, such as the need for accurate and comprehensive data, the difficulty of accounting for complex geological and topographical factors, and the potential for uncertainty in the assessment results.

Carabella et al. (2022) presented a case study on earthquake-induced landslide susceptibility evaluation in the Abruzzo region of Central Italy. The study focused on the use of a statistical approach, the logistic regression model, to analyze the relationship between landslides and various geological, morphological, and land use factors in the study area. He et al. 2021 conducted a study on the use of the random forest (RF) algorithm to assess earthquake-induced landslide susceptibility on a global scale. The research aimed to develop a rapid and accurate method for landslide susceptibility assessment using readily available data. In the study, various factors such as geological, topographical, and anthropogenic factors were employed to train the model. The RF algorithm proved to be a robust tool for the assessment of earthquake-induced landslide susceptibility on a global scale. The study results showed that the developed model has high prediction accuracy, and its outputs are useful for earthquake risk management and mitigation. The study highlights the importance of using the ML

methods for the rapid and accurate assessment of landslide susceptibility on a global scale.

Umar et al. (2014) proposed a combined method for two statistical methods, frequency ratio (FR) and logistic regression (LR), in the production of a landslide susceptibility map in West Sumatra Province, Indonesia. A great number of landslides were triggered in the region during the West Sumatra earthquake (Mw. 7.6). In the study, the susceptibility map was generated with the landslide inventory triggered after the earthquake. In this region, which is susceptible to landslide occurrence, this study was aimed at determining the areas prone to landslides and preventing urbanization and development in these areas. In another study by Zhou et al. (2019), a landslide susceptibility map was produced using the landslides triggered by the Lushan earthquake (Mw. 7.0). The performance of susceptibility maps produced with different statistical and machine learning-based models was compared. Again, in this study, landslides triggered after the earthquake were used in the model training and testing phases. A machine learning-based model provided a more accurate result than models based on statistics.

In the literature, landslide susceptibility maps have often been produced using a single inventory without consideration of seismic events due to a lack of suitable data. Here, unlike most studies, the landslide susceptibility map of the region was produced using the pre-earthquake landslide inventory and tested with the co-seismic landslide inventory that was unseen by the model.

Although categorical ML methods such as decision trees have proven successful in landslide susceptibility mapping (e.g., see Karakas et al., 2020; Can et al., 2021), the validation of the results is still a research area as most studies use a part of the learning data for this purpose. Even though the unused part is not used for model training, the model represents the geological and topographical state of the input data and the landslide inventory. However, extreme events such as the Kahramanmaras earthquakes (6 Feb 2023) push the limit of the model results considering unseen data. Thus, the present study aimed at validating landslide susceptibility mapping using landslides triggered by Kahramanmaras earthquakes (6 Feb 2023). For this reason, we produced the landslide susceptibility map using pre-earthquake landslide inventory with the RF algorithm. In this context, fifteen conditioning parameters were derived from different input datasets. Model performance obtained with the RF algorithm was evaluated with the AUC and statistical metrics. Additionally, feature importance analysis was used to assess the impact of the conditioning parameters on the model. The susceptibility map was also assessed by comparing the landslide susceptibility map and the co-seismic landslide inventory not seen by the model. The methodology (section 2) is explained in the following and the results and discussions (section 3) are provided accordingly. Conclusions and future work are given in the final.

2. METHODOLOGY

2.1 Study Area

On 06 February 2023, two destructive earthquakes with magnitudes of Mw 7.7 and Mw 7.6 occurred, with epicenters in Pazarcik and Elbistan of Kahramanmaras. After the earthquakes, many landslides were triggered and have become one of the most important secondary disasters. Especially, most of these landslides were seen in Amanos Mountains. The study area is located in the southern part of Türkiye as a part of the Amanos mountains with an area of 4,558.50 km². Figure 2 shows the location map of the study area. The area, which is part of the East Anatolian Fault Zone (EAFZ), has strong seismicity and significant tectonic activity. The altitude of the study area varies between 0 and 2,206 m. The slope angles range between 0° and 84°. In addition, there are 33 lithological units in the study area.

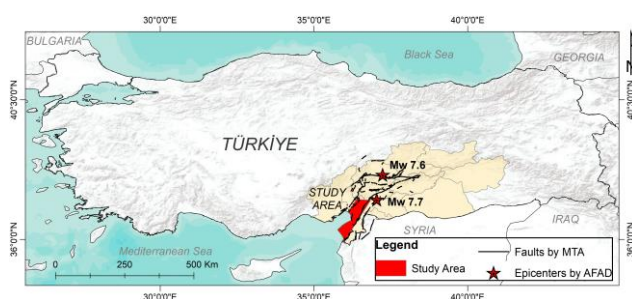


Figure 2. The location map of the study area.

2.1.1. Geological characteristics

Amanos region is one of the most complex and problematic regions of our country in terms of its stratigraphy, structural features and geotectonic location (Yalcin, 1980). The Amanos Mountains lie down on the northwestern edge of the Arabian plate and the Amanos Mountain region was shaped during the evolutionary stages of the Southern Neotethys, containing pre-rift, rift, passive margin, ophiolite formation and emplacement, collision, and uplift (Duman et al., 2017). The Amanos Mountains, which are between the western border of the SE Anatolian Thrust Zone (Emre et al., 2013) and the Karasu-Hatay Graben (Yalcin, 1980) and include the East Anatolian Fault, form the western part of the Eastern Taurus Mountains (Usta et al., 2015). The region has high seismicity, and previous studies (Gokceoglu, 2022; Can et al., 2022) emphasized this character.

The geologic unit in the area was aged from Cambrian to Recent according to a geological map prepared by Ulu (2002). Sedimentary, dynamo metamorphic, volcanic, and ophiolitic rock groups are settled in the region. The stratigraphic series starts with Precambrian-aged meta-sandstones and follows Cambrian to Silurian-aged shelf facies, including sandstone, shale, conglomerates, and carbonate deposits. Shallow water platform carbonates accumulated at the Jurassic age in the region. On top of these geologic units, Late Cretaceous and Miocene-aged ophiolitic rocks were settled. Most of the Paleozoic and Mesozoic sedimentary lithological units were subjected to metamorphism under greenschist facies conditions (Yilmazer and Duman, 1997). It has been stated by Yalcin (1980) that the widely spread ophiolitic rocks in the Amanos Mountains region represent an ancient oceanic crust.

2.1.2. Pre-earthquake and Co-seismic Landslide Inventories

The landslide inventory used in the study is multi-temporal. The pre-earthquake inventory was obtained from the geosciences WebGIS portal of the MTA of Türkiye (MTA, 2023). There were 119 landslides as polygons in the pre-earthquake inventory. The size of the pre-earthquake landslide area coverage ranges from 0.01 km² to 4.31 km². The co-seismic landslide inventory has a total of 619 landslide polygons and was produced in our study by comparing pre-and post-earthquake orthophotos presented on the HGM Küre platform of the General Directorate of Mapping (HGM, 2023). The minimum and maximum post-earthquake landslide area values were calculated as 0.0001 km² and 0.90 km², respectively. Pre-earthquake and co-seismic landslide inventory data together with an altitude map of the study area obtained from the EU-DEM v1.1 of the Copernicus Programme are illustrated in Figure 3. In addition, 3D perspective views of a number of co-seismic landslides are shown on pre- and post-event aerial orthophotos and the pre-event digital elevation model (DEM) in Figure 4.

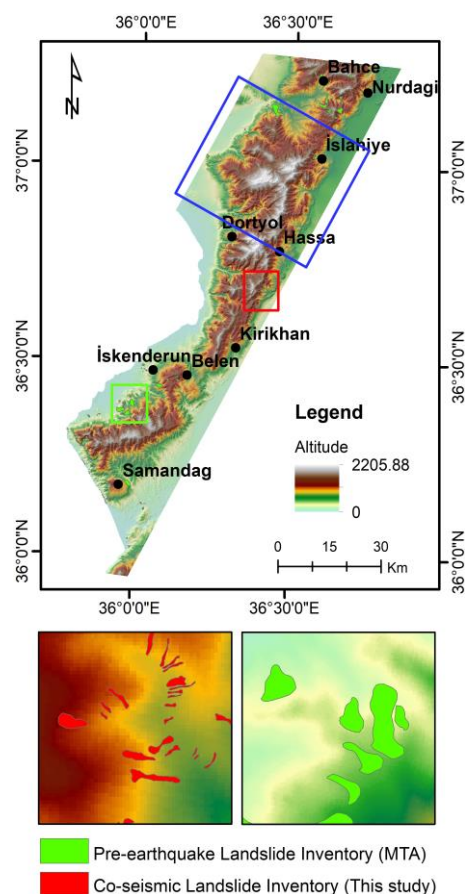


Figure 3. The DEM of the study area with sub-regions selected for further visualization, and parts of the pre-earthquake (green polygon) and co-seismic (red polygon) landslide inventories.

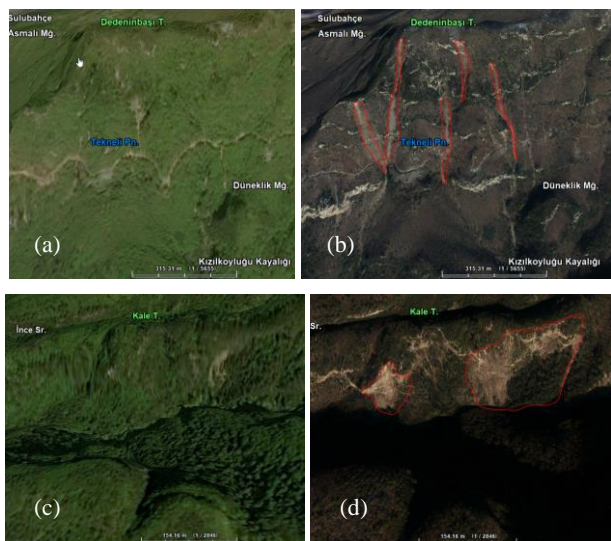


Figure 4. Examples of the co-seismic landslides shown on (a, c) pre-earthquake and (b, d) post-earthquake orthophotos (image credit: HGM Küre).

2.2 Landslide Conditioning Parameters

The study employed 15 conditioning parameters in total. EU-DEM v1.1 was used to acquire topographic characteristics such as altitude, slope, aspect, plan and profile curvatures, topographic wetness index (TWI), stream power index (SPI), strahler order, channel network, and catchment area. These features were frequently used in the literature (e.g., see Gokceoglu and Ercanoglu, 2001; Nefeslioglu et al., 2012; Sevgen et al., 2019; Karakas et al., 2020; Can et al., 2021). EU-DEM stands for “European Digital Elevation Model”. It is a high-resolution DEM that covers the entire European continent and provides topographic information on the Earth’s surface. EU-DEM was developed by the European Environment Agency (EEA) in collaboration with the European Space Agency (ESA) and several European National Mapping Agencies. It is based on the Shuttle Radar Topography Mission (SRTM) DEM and was processed and enhanced to improve its accuracy and quality. EU-DEM is widely used in various applications, including landslide susceptibility mapping, hydrological modeling, and environmental monitoring.

In addition, the distance to roads, rivers, faults, lithological units, and the ESA WorldCover map (ESA-WorldCover, 2020) were used as conditioning factors. The input characteristics and their respective data sources are summarized in Table 1.

Datasets	Data Format	Source	Scale Resolution
EU-DEM v1.1	Grid	The Copernicus Programme	25 m
WorldCover	Grid	ESA	10 m
Lithology	Polygon	MTA	1/100,000
Faults	Polyline	MTA	1/250,000
Roads	Polyline	HGM	1/25,000
Rivers	Polyline	HGM	1/25,000

Table 1. The input features as landslide conditioning factors and their data sources used in the study.

2.3 Landslide Susceptibility Mapping

The RF developed by Breiman (2001) is a popular ML algorithm that has been used in many fields, including geosciences, to predict the likelihood of landslide occurrences. The algorithm works by constructing multiple decision trees based on different subsets of the input data, features, and then combining their predictions to obtain a more accurate and robust model.

In this study, the RF was chosen as a ML algorithm because it has several advantages over the other techniques, such as higher accuracy, robustness to noise and missing data, and the ability to handle high dimensionality with many input variables. It also reduces the risk of overfitting, which is a common problem with decision trees. Additionally, the RF provides flexibility in handling both regression and classification tasks with a high degree of accuracy, and it is effective in feature selection, which can help identify the most important predictors of landslide susceptibility. The RF algorithm was applied here by using the scikit-learn library (Scikit-learn, 2023) in Python.

The pre-earthquake landslide inventory shown in Figure 3 was used for model training and validation. For model training and validation, a total of 7,981 pixels (25 m resolution) available in the landslide inventory were used. 6,384 of those (80%) were used as training data, and the remaining 1597 pixels were used as test data. A total of 11,971 pixels were randomly selected from areas without landslides (50% greater than the inventory). The model’s predictive performance was evaluated with the area under the receiver operatic characteristic curve (AUC), precision, recall and F1 Score values. An external validation was performed by using a co-seismic landslide inventory in the study area. This inventory was never used for model training. For external validation, the susceptibility map and the co-seismic landslide inventory were overlaid and the class values of the pixels under these intersection areas were compared.

The Mean Decrease in Impurity (MDI) method was used to calculate the importance of each predictor variable in the model. The contribution of the predictor variables to the model is taken into account in proportion to the calculated value. The higher the calculated value, the more the parameter contributes to the model.

3. RESULTS AND DISCUSSIONS

In the following, the predictor parameters obtained from the input dataset, the landslide susceptibility map (LSM) produced with the RF algorithm and predictive performance results, and the validation of LSM with co-seismic landslide inventory were assessed and discussed.

3.1 The Predictor Parameters Results

The predictor parameters obtained from the input dataset were classified as topographical (altitude, slope, aspect, plan and profile curvature, catchment area, channel networks and Strahler order), geological (lithology, distance to faults), environmental (LULC, distance to roads), and hydrological (SPI, TWI and distance to rivers). The predictor parameters result of the sub-parts indicated in the blue square in Figure 3 are shown in Figure A1 in the Appendix for visual inspection.

3.2 The LSM, Predictive Performance and Feature Importance Results

Here, the LSM produced with the RF algorithm using fifteen predictor parameters is presented in Figure 5. The result map was classified into five categories (very low, low, moderate, high and very high) using the natural breaks algorithm (Jenks 1967). Table 2 shows the distribution and percentages of landslide probabilities for five categories. These results indicate that more than half of the region is in fact susceptible to landslides.

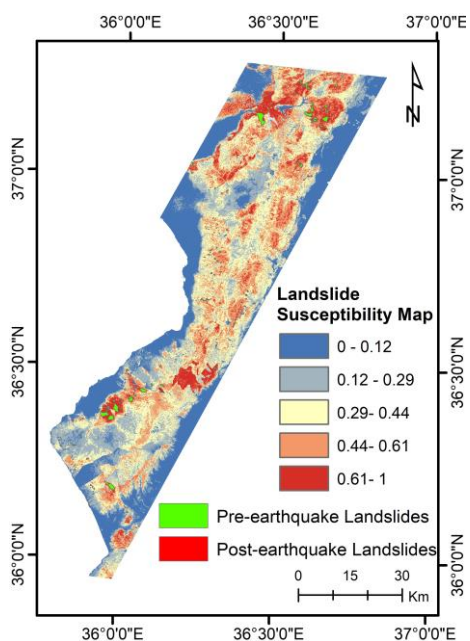


Figure 5. Landslide susceptibility map result using the RF method.

Class	Probability (%)	Size (km ²)	Percentage (%)
Very High	61-100	373.36	8.2
High	44-61	898.64	19.7
Moderate	29-44	1225.52	26.9
Low	12-29	925.68	20.3
Very Low	0-12	1135.29	24.9

Table 2. The landslide probability distributions and percentages obtained from the RF algorithm.

The predictive performance results of the RF algorithm were evaluated according to ROC Curve (AUC value) and statistical measures (F-1 score, precision and overall accuracy value). The ROC Curve obtained from the RF and the statistical metrics results are presented in Figure 6 and Table 3, respectively.

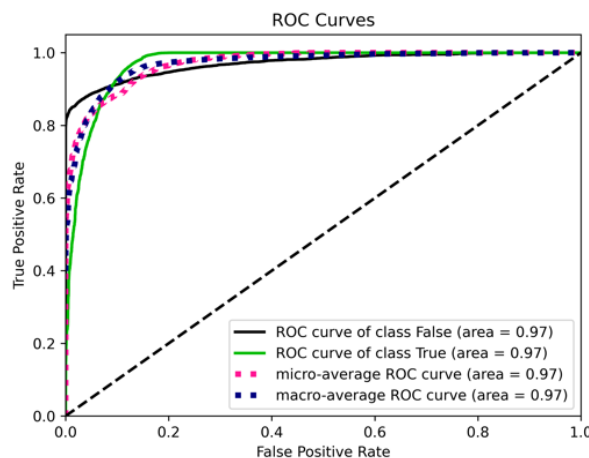


Figure 6. The ROC curve obtained from RF results.

Class	Precision	Recall	F1 Score
Non-landslide	0.98	0.98	0.98
Landslide	0.96	0.97	0.98

Table 3. Overall statistical metrics of the RF algorithm

The importance analysis results of the predictor parameters are given in Figure 7. Slope is the most predictive parameter, followed by lithology, distance to faults, altitude and LULC in the study.

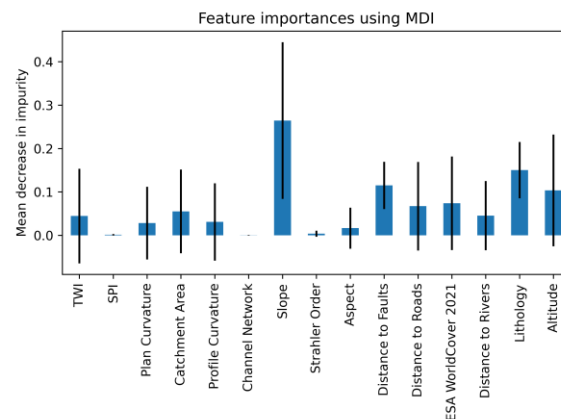


Figure 7. Feature importance results obtained from the RF algorithm.

3.3 Validation of the LSM with Co-seismic Landslides

In this part, the validation of the landslide susceptibility map produced using the RF algorithm was tested using the earthquake-triggered landslide inventory (co-seismic landslides). The test accuracy of the produced landslide susceptibility map has an overall accuracy of 80%. In addition, the results were evaluated visually. In Figure 8, the result of the landslide susceptibility map for some areas is shown together with the co-seismic inventory. It was observed that the landslides triggered after the earthquakes are generally in high-susceptibility areas in the study area.

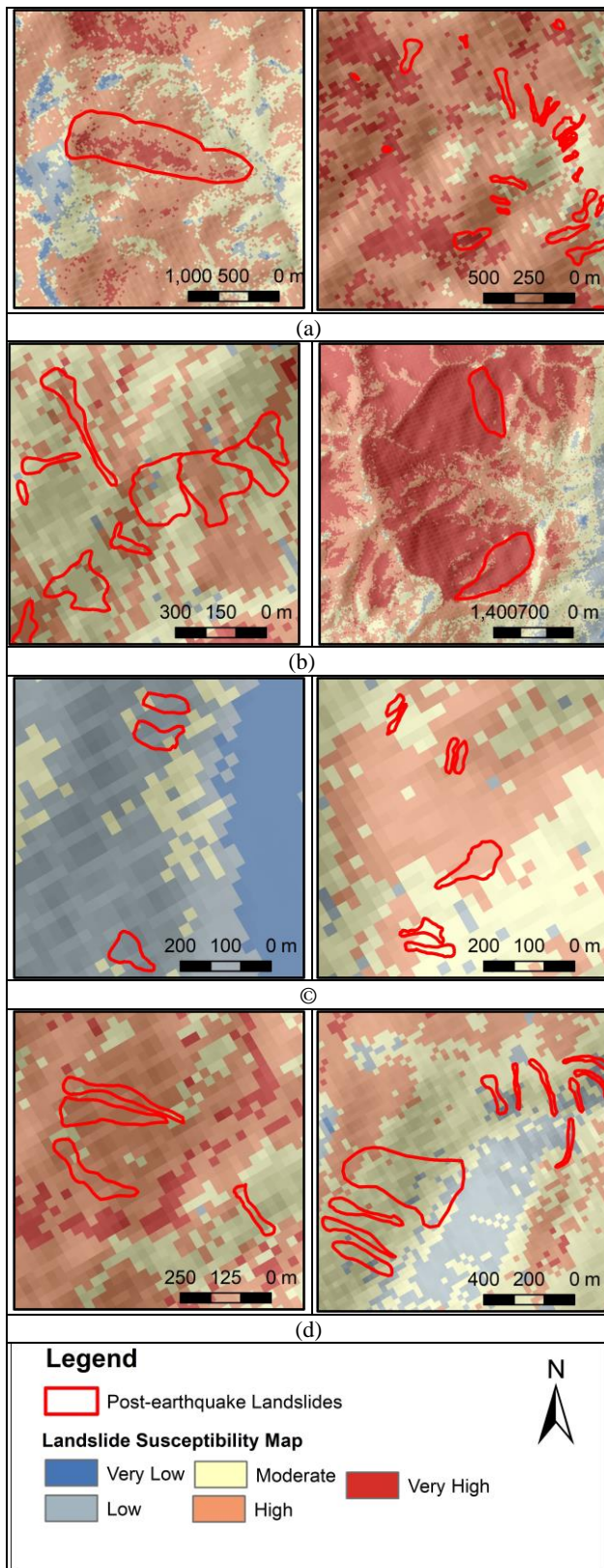


Figure 8. Comparison of the landslide susceptibility map result with the co-seismic landslide inventory (test data) in sub-areas.

4. CONCLUSIONS

In the present study, the validation of RF-based landslide susceptibility mapping was evaluated in a part of the Amanos Mountains. For this evaluation, the landslide inventory triggered after the Kahramanmaraş earthquakes was used. The landslide susceptibility map was produced using the pre-earthquake landslide inventory. The prediction performance of the model evaluated with the AUC value is 97%. The result shows the high classification performance of the RF model for landslide susceptibility and risk assessments. The predictor parameters employed for the landslide susceptibility map were also found suitable for modeling. On the other hand, a co-seismic landslide inventory was used to test the produced landslide susceptibility map. This inventory was never used in the model training phase. The test accuracy result was calculated at 80%.

As can be seen from the pre-earthquake landslide inventory, especially the south part of the Amanos region is free from landslides. However, during the last major earthquakes, several landslides were triggered. This interesting situation shows the importance of regional landslide mapping studies.

The statistically and visually evaluated results show that the produced landslide susceptibility map can contribute to studies such as site selection, sustainable land use planning and future disaster mitigation efforts.

The relationship between pre-earthquake landslide susceptibility analyses and landslides that occur after an earthquake is essential for both pre-disaster planning and post-disaster recovery efforts. Therefore, improving landslide susceptibility maps and studying landslides that occur after an earthquake will be important steps in disaster management.

REFERENCES

- Breiman, L., 2001. Random forests. *Machine learning*, 45, 5-32. <https://doi.org/10.1023/A:1010933404324>.
- Can, R., Kocaman, S., Gokceoglu, C., 2021. A comprehensive assessment of XGBoost algorithm for landslide susceptibility mapping in the upper basin of Ataturk Dam, Turkey. *Applied Sciences*, 11: 4993. <https://doi.org/10.3390/app11114993>.
- Can, A., Baskose, Y., and Gokceoglu, C., 2022. Stability assessments of a triple-tunnel portal with numerical analysis (south of Turkey). *Geotechnical Research*, 9 (2), 116-128. <https://doi.org/10.1680/jgere.21.00028>
- Carabella, C., Cinosi, J., Piattelli, V., Burrato, P., Miccadei, E., 2022. Earthquake-induced landslides susceptibility evaluation: A case study from the Abruzzo region (Central Italy). *CATENA*, 208, 105729. <https://doi.org/10.1016/j.catena.2021.105729>.
- Duman, T.Y., Robertson, A.H.F., Elmacı, H., Kara, M., 2017. Palaeozoic-Recent geological development and uplift of the Amanos Mountains (S Turkey) in the critically located northwesternmost corner of the Arabian continent. *Geodinamica Acta*, 29, 1, 103-138. <https://doi.org/10.1080/09853111.2017.1323428>.
- Emre, Ö., Duman, T.Y., Özalp, S., Elmacı, H., Olgun, Ş., Şaroğlu, Ş., 2013. Active fault map of Turkey with explanatory

text, Ankara, General Directorate of Mineral Research and Exploration, Special Publication Series-30.

ESA-WorldCover, 2020. Worldwide land cover mapping: VITONV.2021. <https://esa-worldcover.org/en> (29 April 2023).

Gokceoglu, C., 2022. Assessment of rate of penetration of a tunnel boring machine in the longest railway tunnel of Turkey. *SN Applied Sciences*, 4, 19. <https://doi.org/10.1007/s42452-021-04903-y>

Gokceoglu, C., Ercanoglu, M., 2001. Heyelan duyarlılık haritalarının hazırlanmasında kullanılan parametrelere ilişkin belirsizlikler. *Yerbilimleri*, 23, 189–206.

He, Q., Wang, M., Liu, K., 2021. Rapidly assessing earthquake-induced landslide susceptibility on a global scale using random forest. *Geomorphology*, 391, 107889. <https://doi.org/10.1016/j.geomorph.2021.107889>.

HGM (General Directorate of Mapping), 2023. HGM Küre Application. URL: <https://hgmkuire.btk.gov.tr/> (last accessed on 29 April 2023).

Jenks, G.F., 1967. The data model concept in statistical mapping. *International Yearbook Cartography*, 7, 186-190.

Karakas, G., Can, R., Kocaman, S., Nefeslioglu, H.A., Gokceoglu, C., 2020. Landslide susceptibility mapping with random forest model for Ordu, Turkey. *ISPRS-International Archives of the Photogrammetry, Remote Sensing and Spatial Information Sciences*, XLIII-B3-2020, 1229–1236. <https://doi.org/10.5194/isprs-archives-XLIII-B3-2020-1229-2020>.

Karakas, G., Nefeslioglu, H.A., Kocaman, S., Buyukdemircioglu, M., Yurur, M.T., Gokceoglu, C., 2021. Derivation of earthquake-induced landslide distribution using aerial photogrammetry: the 24 January 2020 Elazig (Turkey) Earthquake. *Landslides*, 18, 2193-2209. <https://doi.org/10.19111/bulletinofmre.428277>.

Kocaman, S., Tavus, B., Nefeslioglu, H. A., Karakas, G., Gokceoglu, C., 2020. Evaluation of floods and landslides triggered by a meteorological catastrophe (Ordu, Turkey, August 2018) using optical and radar data. *Geofluids*, 12, 1-18. <https://doi.org/10.1155/2020/8830661>.

MTA (General Directorate of Mineral Research and Exploration), 2023. GeoScience Map Viewer. <http://yerbilimleri.mta.gov.tr/> (last accessed on 29 April 2023).

Nefeslioglu, H.A., San, B.T., Gokceoglu, C., Duman, T.Y., 2012. An assessment on the use of Terra ASTER L3A data in landslide susceptibility mapping. *International Journal of Applied Earth Observation and Geoinformation*, 14(1), 40-60. <https://doi.org/10.1016/j.jag.2011.08.005>.

Scikit-learn, 2023. Python Library. <https://scikit-learn.org/stable/> (last accessed on 29 April 2023).

Sevgen, E., Kocaman, S., Nefeslioglu, H.A., Gokceoglu, C., 2019. A Novel Performance Assessment Approach Using Photogrammetric Techniques for Landslide Susceptibility

Mapping with Logistic Regression, ANN and Random Forest. *Sensors*, 19, 3940. <https://doi.org/10.3390/s19183940>.

Shao, X. and Xu, C., 2022. Earthquake-induced landslides susceptibility assessment: A review of the state-of-the-art. *Natural Hazards Research*, 2(3), 172-182. <https://doi.org/10.1016/j.nhres.2022.03.002>.

Ulu, Ü., 2002. 1:500,000 scale Geological map of Turkey, No:16 (Hatay). In M. Şenel (Ed.). General Directorate of Mineral Research and Exploration. Ankara, Turkey.

Umar, Z., Pradhan, B., Ahmad, A., Jebur, M.N. and Tehrani M.S., 2014. Earthquake induced landslide susceptibility mapping using an integrated ensemble frequency ratio and logistic regression models in West Sumatera Province, Indonesia. *Catena*, 118, 124-135. <https://doi.org/10.1016/j.catena.2014.02.005>.

Usta, D., Ateş, Ş., Beyazpınar, M., Kanar, F., Yıldız, H., Uçar, L., Akça, İ., Tufan, E., Örtlek, A.T., 2015. New Data On The Stratigraphy Of The Central And Northernamonus Mountains (Osmaniye – Gaziantep – K.Maraş). *TAPG Bulletin*, Volume 27, No 1, Page 57-98.

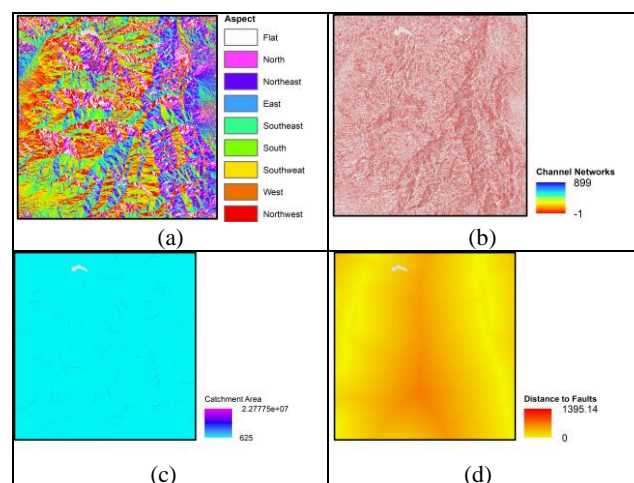
Yanar, T., Kocaman, S., Gokceoglu, C., 2020. Use of Mamdani fuzzy algorithm for multi-hazard susceptibility assessment in a developing urban settlement (Mamak, Ankara, Turkey). *ISPRS International Journal of Geo-Information*, 9 (2), 114. <https://doi.org/10.3390/ijgi9020114>.

Yalcin, N., 1980. The lithological characteristics of the Amanos and their sense in the tectonic evolution of Southeast Anatolia. *Bulletin of the Geological Society of Turkey*, 25, 21–30.

Yilmazer, İ., Duman, T.Y., 1997. Geotechnical problems arising from the incorrect nomenclature of the units forming Nurdağ. *Yerbilimleri*, 30, 341–349.

Zhou, S., Zhang, Y., Xing, J., Chen, C., and Fang, L., 2019. Earthquake-induced landslide susceptibility mapping: Application and Comparison of Frequency Ratio, Logistic Regression, Weight of Evidence and Support Vector Machine. *IOP Conf. Ser.: Earth Environ. Sci.*, 304, 042011. <https://doi.org/10.1088/1755-1315/304/4/042011>.

APPENDIX



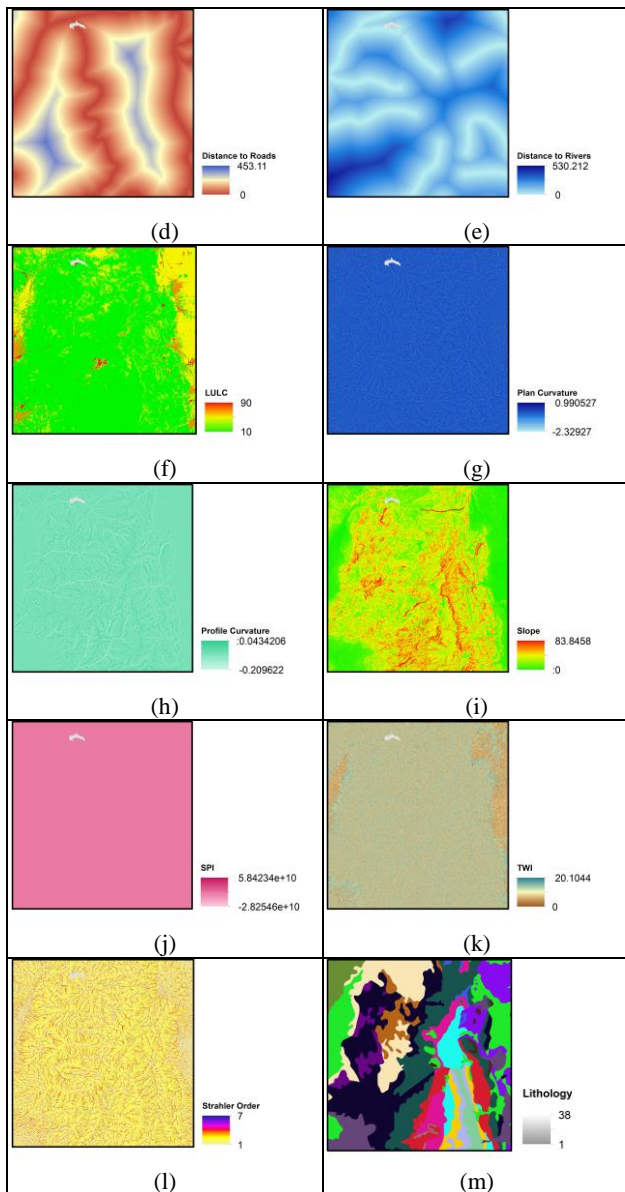


Figure A1. The landslide conditioning parameters used in the study.